Res Chem Intermed (2018) 44:5801–5815
https://doi.org/10.1007/s11164-018-3456-3

Sulfonated chitosan-encapsulated HAp@Fe_3O_4: an efficient and recyclable magnetic nanocatalyst for rapid eco-friendly synthesis of 2-amino-4-substituted-1,4-dihydrobenzo[4, 5]imidazo[1,2-a] pyrimidine-3-carbonitriles

Vilas N. Mahire[1,2] · Girish P. Patil[3,4] · Amol B. Deore[3] · Padmakar G. Chavan[3] · Harishchandra D. Jirimali[1] · Pramod P. Mahulikar[1]

Received: 13 February 2018 / Accepted: 24 April 2018 / Published online: 4 May 2018

Abstract A one-pot, multi-component, synthetic method for preparation of 2-amino-4-substituted-1,4-dihydrobenzo[4,5]imidazo[1,2-a]pyrimidine-3-carbonitriles has been developed. It was accomplished by mixing 2-aminobenzimidazole, aldehyde and malononitrile in the presence of S-Chit-HAp@Fe_3O_4 as a nanocatalyst in aqueous medium. The catalyst (S-Chit-HAp@Fe_3O_4) was synthesized using a co-precipitation method and further characterized by using FT-IR, XRD, FE-SEM, EDX, HR-TEM, TGA and VSM analysis. It was found that the catalyst exhibits magnetic properties and showed high catalytical activity for the synthesis of 2-amino-4-substituted-1,4-dihydrobenzo[4,5]imidazo[1,2-a]pyrimidine-3-carbonitriles.

Electronic supplementary material The online version of this article (https://doi.org/10.1007/s11164-018-3456-3) contains supplementary material, which is available to authorized users.

✉ Pramod P. Mahulikar
mahulikarpp@gmail.com

[1] School of Chemical Sciences, North Maharashtra University, Jalgaon, Maharashtra, India

[2] Department of Chemistry, Bhusawal Arts, Science and P. O. Nahata Commerce College, Bhusawal, Maharashtra, India

[3] School of Physical Sciences, North Maharashtra University, Jalgaon, Maharashtra, India

[4] SVKM's Institute of Technology, Dhule, India

Graphical Abstract S-Chit-HAp@Fe_3O_4 nanoparticles catalyzing one-pot, multi-component synthesis of 2-amino-4-substituted-1,4-dihydrobenzo[4,5]imidazo[1,2-a]pyrimidine-3-carbonitriles in aqueous medium has been reported herein.

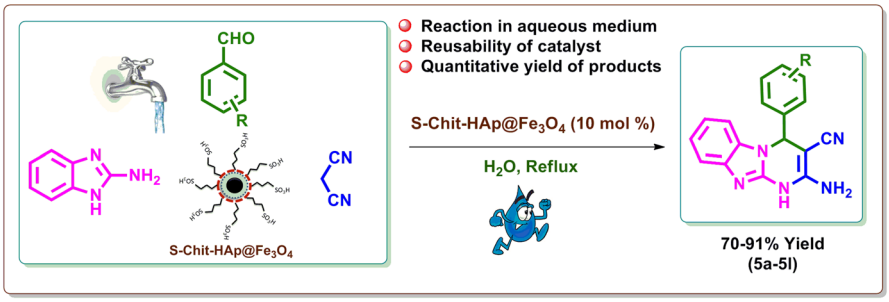

Keywords Green chemistry · S-Chit-HAp@Fe_3O_4 · Chitosan · Hydroxyapatite · Fe_3O_4 nanoparticles · 2-Aminobenzimidazole · Malononitrile

Introduction

The development of greener protocols for the synthesis of highly functionalized motifs having medicinal value is always a welcome in pharmaceutical science and is an attractive research thrust area. In organic synthesis, multi-component reactions are highly desirable because the rapid generation of complex molecules is achieved in a single reaction step through the appropriate combination of three or more substrates in a single reaction flask and by avoiding the intermediate steps. The diversity-oriented organic synthesis or drug designing are the best examples of multi-component reactions [1, 2]. It is well known that pyrimidinobenzimidazoles have a wide range of biological activities such as antimicrobial [3], antiulcer [4], anti-HIV [5] and antiviral activity [6], etc. Furthermore, pyrimidinobenzimidazoles are also found to be better analgesic, anti-inflammatory and antiamoebic drugs [7].

Nowadays, magnetic nanoparticles have opened a new avenue as powerful and clean recoverable supports for a variety of organic transformations, since they could be easily separated by an external magnetic field [8]. The Fe_3O_4 nanoparticles are hydrophilic in nature and are able to aggregate into large clusters. Therefore, surface modification is an appropriate strategy to prevent agglomeration of nanoparticles [9–12]. As per the literature, it is found that hydroxyapatite [$Ca_{10}(PO_4)_6(OH)_2$] is an ideal material for encapsulating iron oxide nanoparticles. It is a biocompatible inorganic nanomaterial used for preparation of a high-performance heterogeneous catalyst [13, 14]. Recently, nanoparticles made from natural materials, particularly polysaccharides, have attracted attention as environmentally benign polymeric supports [15–18]. Among biopolymers, chitosan is an excellent support material for catalytic applications in heterogeneous catalysis reaction. Moreover, chitosan is used as an environmentally benign polymeric support due to its excellent chelating

and mechanical properties. The terminal hydroxyl and amino groups of chitosan can be suitably modified to anchoring sites for catalytical applications [19–21].

As per the reports, non-magnetic nanoparticles have disadvantages like loss of catalytic ability during centrifugation and filtration processes. Hence, we decided to synthesize the magnetic nanoparticles since they can be simply separated from a reaction mass by an external magnet and recycled for subsequent reactions. Fe_3O_4 nanoparticles are easily oxidized in atmosphere; hence, modification of their surface is an essential task. Therefore, hydroxyapatite and then chitosan were grafted over the surface of Fe_3O_4 nanoparticles to achieve additional porosity and stability. Furthermore, the catalyst was then sulfonated using 1, 3-propane sultone to obtain additional active sites for the catalyst. The strategy for preparing the catalyst is summarized in Scheme 1. The synthesized nanocatalyst was found to be efficient and a recyclable support for one-pot, multi-component synthesis of 2-amino-4-substituted-1,4-dihydrobenzo[4,5]imidazo[1,2-a]pyrimidine-3-carbonitriles in aqueous media (Scheme 2). In continuation of our work on synthesis of bioactive compounds using green chemistry [22–24], we have attempted in the present work a cleaner synthesis using newly developed magnetic catalyst.

Results and discussion

FT-IR analysis

In FT-IR spectral study (Fig. 1), Fig. 1a represents FT-IR spectrum of Fe_3O_4 nanoparticles, in which the characteristic vibration band observed at 583 cm^{-1} was due to the Fe–O vibration and the bands at 3391 and 1622 cm^{-1} were due to adsorbed water molecules. The FT-IR spectrum of HAp@Fe_3O_4 nanoparticles

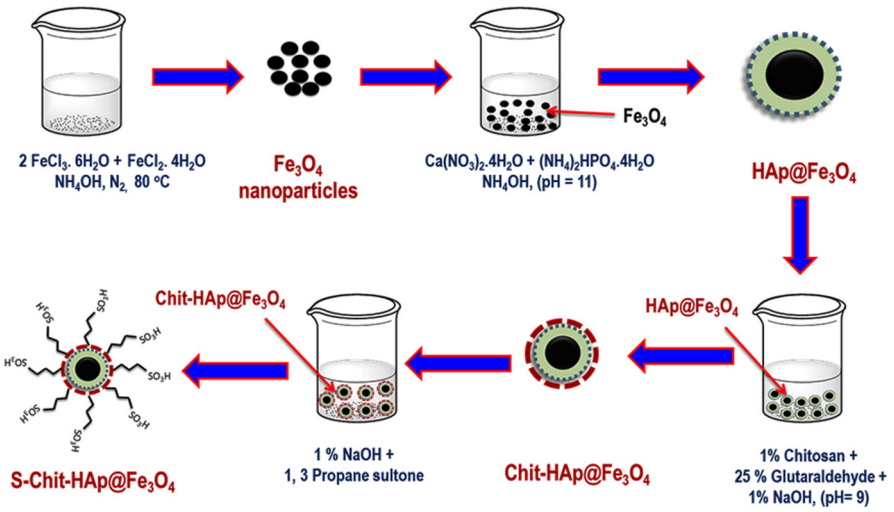

Scheme 1 Schematic visualization for preparation of S-Chit-HAp@Fe_3O_4 nanoparticles

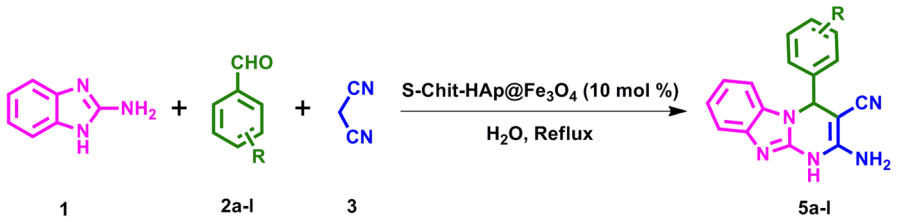

Scheme 2 Synthesis of 2-amino-4-substituted-1,4-dihydrobenzo[4,5]imidazo[1,2-a]pyrimidine-3-carbonitrile derivatives

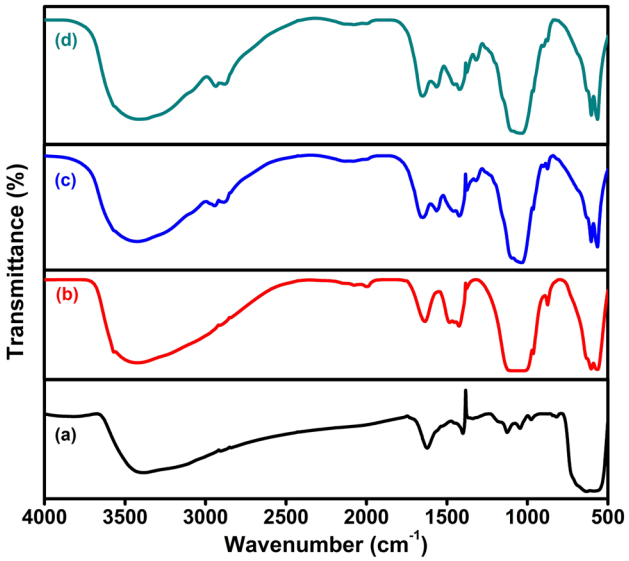

Fig. 1 FT-IR spectra of (a) Fe_3O_4, (b) HAp@Fe_3O_4, (c) Chit-HAp@Fe_3O_4 and (d) S-Chit-HAp@Fe_3O_4

(Fig. 1b) showed broad bands at 3424 and 1636 cm^{-1} due to stretching and bending vibrations of molecularly adsorbed water molecules. Also, the stretching vibration at around 3567 cm^{-1} confirmed the presence of hydroxyl groups. The symmetric stretching vibrations of the PO_4^{3-} ion were also found at around 1043 and 962 cm^{-1}. The absorption bands at 603 and 563 cm^{-1} were attributed to asymmetric stretching and bending vibration frequencies of the PO_4^{3-} ion, respectively. The above results indicated successful grafting of HAp over Fe_3O_4 nanoparticles. Figure 1c shows the FT-IR spectrum of Chit-HAp@Fe_3O_4 nanoparticles in which broad peaks near 3424 cm^{-1} could be attributed to the N–H and O–H stretching vibrations, as well as inter- and extra-molecular hydrogen bonding existing in chitosan skeletons [25]. There could also the contribution of an $–NH_2$ absorption band in the region of 3400–3000 cm^{-1}, which was found to be merged by the O–H stretching vibrations. The weak band near 2884 cm^{-1} was attributed to the C–H stretching vibration. The band at 1647 cm^{-1} was assigned to N–H bending vibration and that of 1423 cm^{-1} to C–O stretching of primary alcoholic groups in

chitosan. Figure 1d represents FT-IR spectrum of S-Chit-HAp@Fe_3O_4 nanoparticles with absorption bands at 1377 and 1035 cm^{-1} corresponding to the stretching vibration of the S=O group, and the bands appearing at 2881 cm^{-1} were characteristic of C–H stretching vibrations, indicating successful sulfonation of Chit-HAp@Fe_3O_4 nanoparticles. Therefore, FT-IR spectral data confirmed the successful encapsulation of Fe_3O_4 nanoparticles with hydroxyapatite, chitosan and 1, 3-propane sultone layers.

XRD analysis

The XRD analysis was carried out to gain evidence of Chit-HAp as well as Fe_3O_4 nanoparticles and also for determining the crystallographic features. In XRD patterns (Fig. 2), the diffraction peaks of Fe_3O_4 were noted at 30.4°, 35.5°, 43.5°, 53.7°, 57.5° and 63°. These peaks were indexed to the cubic crystalline structure of Fe_3O_4 with an Fd3/m space group and lattice parameter $a = b = c = 8.398$ Å (JCPDS card no. # 79-0418), which confirmed the formation of Fe_3O_4 phase. Additionally, the diffraction peaks found in case of HAp@Fe_3O_4, Chit-HAp@Fe_3O_4 and S-Chit-HAp@Fe_3O_4 were indexed to the hydroxyapatite with an P63/m space group and lattice parameters $a = 9.439$ Å and $c = 6.886$ Å (JCPDS card no. #

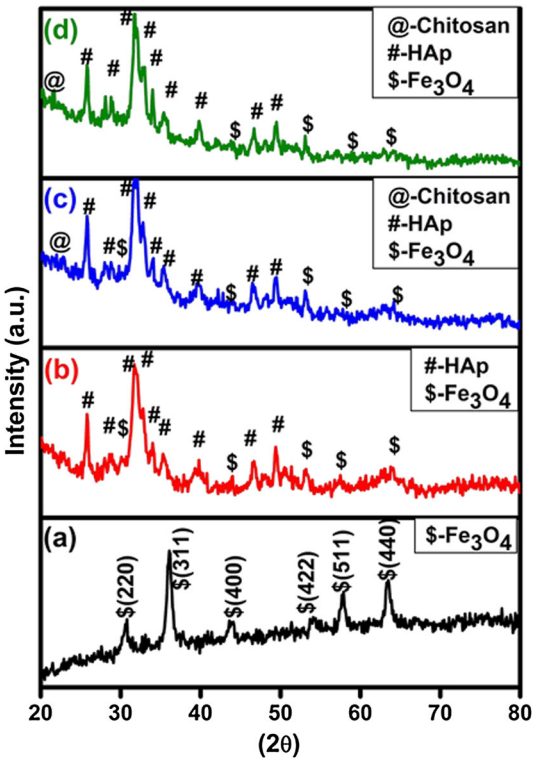

Fig. 2 XRD patterns of (a) Fe_3O_4, (b) HAp@Fe_3O_4, (c) Chit-HAp@Fe_3O_4 and (d) S-Chit-HAp@Fe_3O_4

896438). In the XRD patterns of Chit-HAp@Fe_3O_4 and S-Chit-HAp@Fe_3O_4, the small diffraction peaks of chitosan centred at 20.4° were observed [26].

FE-SEM and EDX analysis

FE-SEM images of Fe_3O_4, HAp@Fe_3O_4, Chit-HAp@Fe_3O_4 and S-Chit-HAp@Fe_3O_4 are depicted in Fig. 3. Figure 3a shows the FE-SEM image of Fe_3O_4 nanoparticles with an average diameter of 11 nm. An FE-SEM image of HAp@Fe_3O_4 nanoparticles is shown in Fig. 3b which visualises the formation of nanoparticle as well as the nanorod-like morphology of HAp@Fe_3O_4 (shown by the arrow). Figure 3c indicates the gel-like coating of chitosan over the HAp@Fe_3O_4 nanoparticles/nanorods, confirming the formation of Chit-HAp@Fe_3O_4 nanoparticles. Figure 3d shows thr explored S-Chit-HAp@Fe_3O_4 configuration formed after sulfonation. Figure S22 shows the EDX spectrum of S-Chit-HAp@Fe_3O_4 nanoparticles in which the characteristic peaks of Fe, Ca, N, O and S were observed and that confirmed the successful grafting of layers over Fe_3O_4 nanoparticles.

TEM analysis

To study the morphology and crystalline nature of S-Chit-HAp@Fe_3O_4 matrix, detailed TEM characterizations were carried out. The bright field images of S-Chit-HAp@Fe_3O_4 matrix are shown in Fig. 4a and b. The close-up image of S-Chit-HAp@Fe_3O_4 matrix is shown in Fig. 4b, from which we noted the formation of the

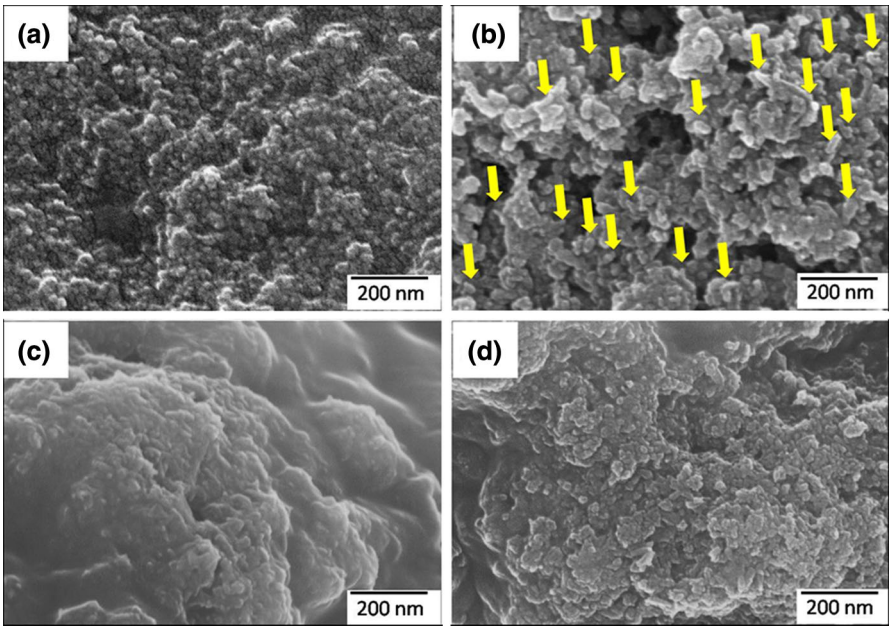

Fig. 3 FE-SEM images of **a** Fe_3O_4, **b** HAp@Fe_3O_4, **c** Chit-HAp@Fe_3O_4 and **d** S-Chit-HAp@Fe_3O_4

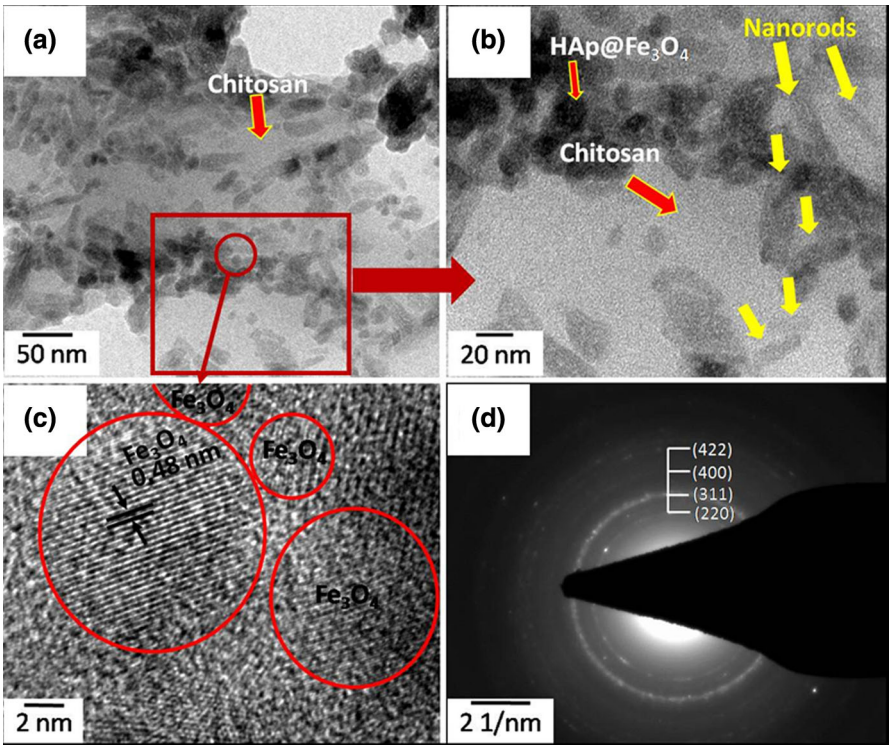

Fig. 4 **a** and **b** TEM images of S-Chit-HAp@Fe_3O_4 matrix, **c** HRTEM images of S-Chit-HAp@Fe_3O_4 matrix, **d** selected area electron diffraction pattern of S-Chit-HAp@Fe_3O_4 matrix

rod-like structure of HAp@Fe_3O_4 with an average diameter of 10 nm (shown by the arrow). Figure 4c depicts an HR-TEM image of S-Chit- HAp@Fe_3O_4 matrix, which revealed that an individual Fe_3O_4 nanoparticle has a single-crystalline nature with a fringe spacing of 0.48 nm [27]. The selected area electron diffraction (SAED) pattern is shown in Fig. 4d which indicates the polycrystalline nature of the Fe_3O_4.

TGA

TGA analysis of the newly synthesized material, S-Chit-HAp@Fe_3O_4 and its step-by-step buildup from Fe_3O_4, is depicted in Fig. 5. The TGA curves of Fe_3O_4, HAp@Fe_3O_4, Chit-HAp@Fe_3O_4 and S-Chit-HAp@Fe_3O_4 nanoparticles were obtained in N_2 atmosphere in the dynamic mode starting from room temperature to 800 °C. TGA curves of Fe_3O_4 and HAp@Fe_3O_4 nanoparticles (Fig. 5a, b) did not show any considerable weight loss. The small amount of weight loss was observed due to the elimination of adsorbed moisture and condensation of the peripheral hydroxyl groups, which was around 3–4%. The Chit-HAp@Fe_3O_4 (Fig. 5c) was prepared by grafting of organic bio-polymer chitosan on the inorganic HAp@Fe_3O_4 nanoparticles and, hence, the grafted chitosan polymer showed elimination of free NH_2 and OH terminal groups of chitosan and the degradation started at around 180–420 °C with

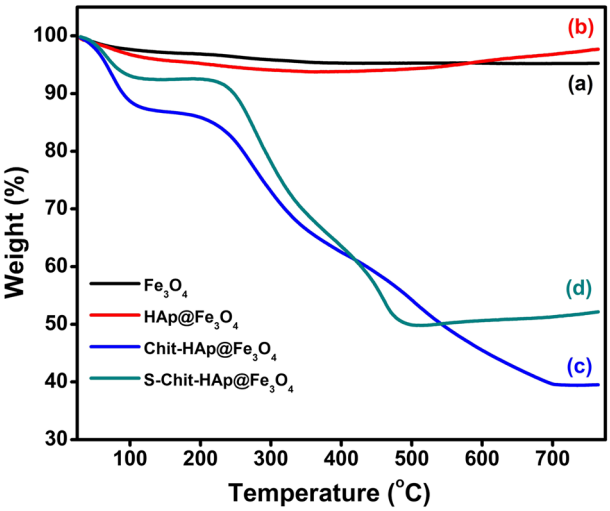

Fig. 5 TGA thermograms of (a) Fe_3O_4, (b) HAp@Fe_3O_4, (c) Chit-HAp@Fe_3O_4 and (d) S-Chit-HAp@Fe_3O_4

total weight loss of 25.29%. The degradation observed at 420–765 °C was due to the pyrolysis of the cross-linked sugar units and of which the weight loss amounts to 21.90%. The TGA curve of S-Chit-HAp@Fe_3O_4 (Fig. 5d) in the temperature range of 180–500 °C showed the elimination of the sulfonated free chains of the modified chitosan with a smaller weight loss as compared to the Chit-HAp@Fe_3O_4 due to the increased extent of organic content of the material. The amount of residue of the pyrolyzed material remaining at 500–700 °C was found to be more in case of S-Chit-HAp@Fe_3O_4 than that for Chit-HAp@Fe_3O_4.

VSM analysis

Figure 6 shows VSM curves in which Fe_3O_4 showed the highest saturation magnetization. The drastic decrease in saturation magnetization from 1.712 to 0.157 memu was observed when HAp was coated over Fe_3O_4. Furthermore, HAp@Fe_3O_4 was coated with chitosan and its saturation was found to decreases again to 0.061 memu. On sulfonation of Chit-HAp@Fe_3O_4, the magnetization value decreased to 0.056 memu. In summary, the continuous decreasing trend in magnetization value upon coating confirmed the successful coating of Fe_3O_4 and the coating thickness was found to be increasing with coatings of different coaters.

Optimization of reaction conditions

In the preliminary attempts at optimizing the reaction conditions, we initially carried out a model reaction of 2-aminobenzimidazole **1** (2 mmol), 4-chlorobenzaldehyde **2a** (2 mmol) and malononitrile **3** (2 mmol) in the presence of S-Chit-HAp@Fe_3O_4 (5 mol%) as a catalyst in water (5 mL) under reflux condition for 15 min, and we

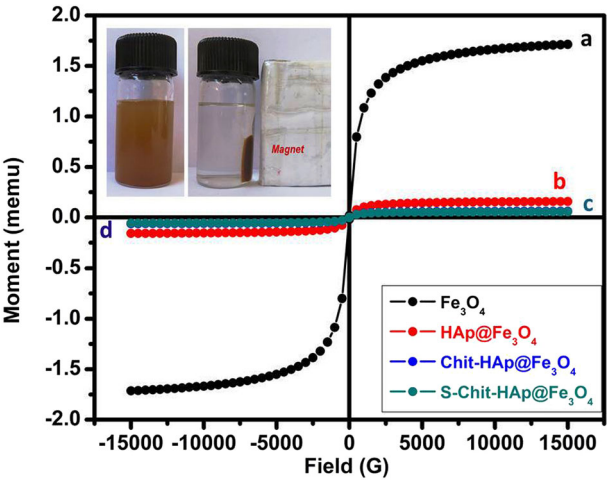

Fig. 6 Magnetization curves of **a** Fe_3O_4, **b** HAp@Fe_3O_4, **c** Chit-HAp@Fe_3O_4 and **d** S-Chit-HAp@Fe_3O_4

obtained product **5a** with a 76% yield (Table 1, entry 2). In order to optimize the reaction conditions, the model reaction was screened for the effect of solvents and quantity of catalyst loading. The reaction in water using 10 mol% of catalyst was found to offer the optimized reaction condition for synthesis of pyrimidinobenzimidazoles (Table 2, entry 10). It was found that there was non-significant loss in catalytic activity of the catalyst even after a third reaction cycle.

Initially, model reactions were performed in solvents like dichloromethane, dimethylformamide and chloroform in reflux conditions; however, no satisfactory yield of **5a** was obtained (Table 2, entries 1, 2 and 4). Furthermore, the reactions in acetonitrile and ethanol resulted in moderate yields (**5a,** Table 2, entries 3 and 5). The model reaction was further examined for effect of temperature on rate of reaction and it was observed that the period and yield of reactions were dependent

Table 1 Reaction of 2-aminobenzimidazole **1**, 4-chlorobenzaldehyde **2a** and malononitrile **3** in the presence of S-Chit-HAp@Fe_3O_4

Entry	Catalyst (mol%)	Time (min)	Yield of 5a[a] (%)
1	None	8 (h)	52
2	5	15	76
3[b]	10	15	88, 83, 83
4	15	15	79
5	20	15	65

Conditions: 2-aminobenzimidazole **1** (2 mmol), 4-chlorobenzaldehyde **2a** (2 mmol), malononitrile **3** (2 mmol)

[a]Isolated yields

[b]Catalyst was reused three times

Table 2 Reaction of 2-aminobenzimidazole **1**, 4-chlorobenzaldehyde **2a** and malononitrile **3** in different solvents

Entry	Solvent	Temp (°C)	Time (min)	Yield of 5a[a] (%)
1	CH_2Cl_2	Reflux	240	37
2	$CHCl_3$	Reflux	240	52
3	CH_3CN	Reflux	180	62
4	DMF	100	240	43
5	C_2H_5OH	Reflux	60	73
6	C_2H_5OH: H_2O (50:50)	Reflux	60	58
7	C_2H_5OH: H_2O (20:80)	Reflux	30	81
8	H_2O	RT	180	Trace
9	H_2O	60	180	72
10	H_2O	Reflux	15	88

Conditions: 2-aminobenzimidazole **1** (2 mmol), 4-chlorobenzaldehyde **2a** (2 mmol), malononitrile **3** (2 mmol) and S-Chit-HAp@Fe_3O_4 nanoparticles (10 mol%)

[a]Isolated yields

on solvent rather than temperature (Table 2, entries 8 and 9). Shaabani et al. attempted synthesis of pyrimidinobenzimidazoles in water [28] and reported that reactions required 7–12 h for completion with only 70% yield of **5a**; however, in the present work, the same reaction catalyzed by 10 mol% of catalyst (S-Chit-HAp@Fe_3O_4) in water was completed within only 15 min with better yield of **5a** (88%). This result confirmed an anchoring support of catalyst to promote the reaction within a shorter period with maximum yield of product.

Once reaction was identified, the scope and limitations of the developed synthetic protocol were further explored under the optimized reaction conditions with aldehydes having different substituents (Table 3). Among all these studied cases, better yields of the desired products were obtained within short reaction time. It was observed that an electron-withdrawing group in the aldehyde boosted the reaction with higher yield, while the electron-donating group reflected a somewhat opposite effect.

It is well known that water is non-toxic, inexpensive, universal as well as green solvent and, thus, reactions in water medium have gained considerable interest. The present study also reinforced the importance of water as a solvent in green chemistry. The catalyst exhibited remarkable activity irrespective of the groups in aldehydes to boost the reactions towards better yields within a short period (Scheme 3).

Proposed mechanism

The reaction presumably proceeds in three steps (Scheme 4), initial condensation of aldehyde **2** and malononitrile **3** by Knoevenagel condensation to form an intermediate called arylidene malononitrile (I). It is then followed by Michael type

Table 3 Synthesis of 2-amino-4-substituted-1,4-dihydrobenzo[4,5]imidazo[1,2-a]pyrimidine-3-carbonitrile[a]

Entry	R	Product	Time (min)	Yield (%)[b]	M.p. (°C)		References
					Found	Reported	
1	4-ClC_6H_4	**5a**	10	88	226	234–236	[30–33]
2	2-FC_6H_4	**5b**	10	75	208–210	224–226	[30–33]
3	2-ClC_6H_4	**5c**	08	83	222–224	236–238	[30–33]
4	4-FC_6H_4	**5d**	10	79	218	266–268	[30–33]
5	4-$CH_3C_6H_4$	**5e**	15	70	200	–	–
6	2-F, 4-ClC_6H_3	**5f**	30	91	212	–	–
7	2,5-$(OCH_3)_2C_6H_3$	**5g**	90	90	216	–	–
8	2-BrC_6H_4	**5h**	15	91	214	–	–
9	3-BrC_6H_4	**5i**	15	85	208	238–240	[30–33]
10	4-BrC_6H_4	**5j**	20	89	210	317–319	
11	3-$NO_2C_6H_4$	**5k**	15	81	218	236	[28]
12	4-CNC_6H_4	**5l**	12	70	222	–	–

[a]General reaction conditions: 2-aminobenzimidazole **1** (2 mmol), aldehydes **2a-l** (2 mmol), malononitrile **3** (2 mmol), S-Chi-HAp@Fe_3O_4 nanoparticles (10 mol%) and H_2O (5 mL)

[b]Isolated yields

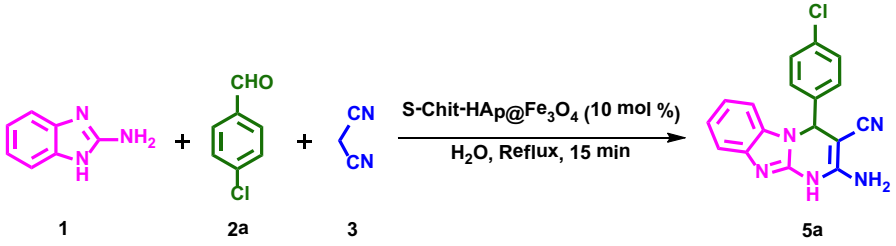

Scheme 3 Optimization of reaction conditions

addition between 2-aminobenzimidazole **1** and arylidene malononitrile **I** to give unstable intermediate **II**, which undergoes intramolecular cyclization affording the desired product 2-amino-4-substituted-1,4-dihydrobenzo[4,5]imidazo[1,2-a]pyrimidine-3-carbonitriles.

Experimental

Materials and methods

All the solvents and reagents were purchased from commercial suppliers, Sigma-Aldrich Ltd., S. D. Fine Chemicals Ltd., Spectrochem India Ltd., and were used

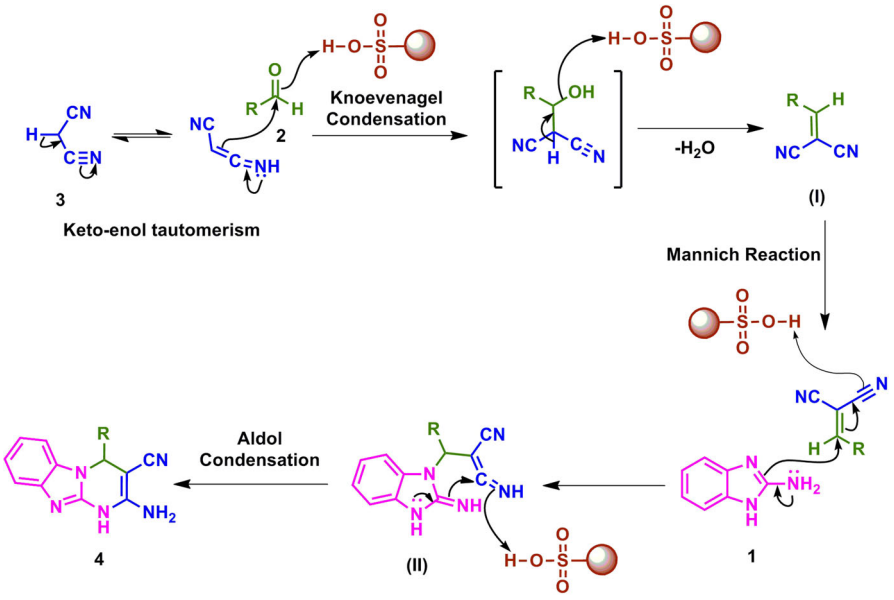

Scheme 4 Proposed mechanism for synthesis of 2-amino-4-substituted-1,4-dihydrobenzo[4,5]imidazo[1,2-a]pyrimidine-3-carbonitrile derivatives

without further purification. The progress of each reaction was monitored by thin layer chromatography (TLC) on 0.2-mm precoated silica gel 60 F254 plates (Merck, Germany) with spots located using UV light as the visualizing agent. Melting points were obtained by an open capillary method and are uncorrected. The IR spectra (KBr pellets) were recorded on Perkin Elmer FT-IR C88522 spectrophotometer. The ^{1}H NMR and ^{13}C NMR spectra were recorded on FT-NMR Bruker Avance-II spectrometer at 400 and 100 MHz, respectively, using DMSO-d_6 as a solvent. The mass spectra were recorded on a Waters Q-Tof Micromass (LCMS) spectrometer in electrospray ionization (ESI) mode. The X-ray diffractograms (XRD) of the catalyst were recorded in the range of 20–80 on a Bruker D8-Advance instrument. The FE-SEM analysis of the catalyst was performed on a Hitachi S-4800 scanning electron microscope (Japan) with an accelerating voltage of 30 kV. The EDX analysis of catalyst was performed by using Bruker EDX flash detector mode 5030. The field emission gun transmission electron microscopy (FEG-TEM, 300 kV) of the catalyst was performed on an FEI Tecnai G2 F30 instrument. TGA data were obtained with a Perkin Elmer instrument in the temperature range of 29–800 °C at a constant heating (10 °C/min) in a nitrogen atmosphere (20 mL/min). The magnetization curves of the samples were measured at room temperature with a Lake Shore 7410 vibrating sample magnetometer (VSM).

Preparation of Fe_3O_4 nanoparticles

Fe_3O_4 magnetic nanoparticles were synthesized by co-precipitation of $FeCl_3{\cdot}6H_2O$ and $FeCl_2{\cdot}4H_2O$ in ammonia solution, according to the reported procedure [29]. Typically, $FeCl_3{\cdot}6H_2O$ (2.7 g, 10 mmol) and $FeCl_2{\cdot}4H_2O$ (0.99 g, 5 mmol) were dissolved in 100 mL of distilled water at 80 °C under N_2 atmosphere and vigorous stirring. Then, 7.5 mL of 25% NH_4OH solution was added to the reaction mixture in one portion with vigorous mechanical stirring. Addition of NH_4OH to the Fe^{2+}/Fe^{3+} salt solution resulted in immediate precipitation of the ferric hydroxide. After 1 h, the mixture was cooled to room temperature, and the resulting black precipitate was separated by applying an external magnet, washed four times with distilled water and heated in vacuum at 110 °C for 4 h to obtain the particles in Fe_3O_4 form.

Preparation of magnetic hydroxyapatite nanoparticles (HAp@Fe_3O_4)

In a 250-mL round-bottom flask, Fe_3O_4 nanoparticles (409 mg) were added to a solution of $Ca(NO_3)_2{\cdot}4H_2O$ (7.59 g, 33.7 mmol) in 50 mL of water, and the reaction mass was stirred at room temperature. $(NH_4)_2HPO_4{\cdot}4H_2O$ (2.64 g, 20 mmol) in 50 mL of water was added drop-wise (1 mL/min) to the above solution and the pH of the resulting solution was adjusted to 11. The total mass was stirred for 2 h and then aged for 24 h. The obtained precipitate was separated by a magnet, washed repeatedly with deionized water to make it neutral and then dried in oven at 110 °C overnight to obtain HAp@Fe_3O_4 nanoparticles.

Preparation of chitosan-coated magnetic hydroxyapatite nanoparticles (Chit-HAp@Fe_3O_4)

In order to coat chitosan onto the surface of HAp@Fe_3O_4, 1 g of chitosan was dissolved in 100 mL of 1% acetic acid solution in a 250-mL beaker containing 1 g of prepared HAp@Fe_3O_4. Subsequently, 2.6 mL of 25% glutaraldehyde solution was added into the mixture. The mixed solution was stirred continuously by a homogenizer for 30 min in order to disperse HAp@Fe_3O_4 nanoparticles into chitosan solution. Chitosan reacts with glutaraldehyde to form cross-link hydrogel. The pH in the system was adjusted to 9 using 1% NaOH solution. The mixture was stirred and homogenized for 2 h at room temperature, resulting in the formation of Chit-HAp@Fe_3O_4 nanoparticles. The synthesized nanoparticles were filtered, washed with distilled water and dried in an oven at 110 °C overnight to obtain Chit-HAp@Fe_3O_4 nanoparticles.

Sulfonation of chitosan-coated magnetic hydroxyapatite nanoparticles (S-Chit-HAp@Fe_3O_4) (Scheme 1)

Chit-HAp@Fe_3O_4 nanoparticles (750 mg) were added to the 1% NaOH solution (100 mL) in a 250-mL round-bottom flask and stirred for 10 min. To this solution, 1, 3-propane sultone (305 mg) was added and refluxed for 6 h. The resulting

product was filtered, washed with distilled water and dried in an oven at 110 °C for 4 h.

General procedure for synthesis of 2-amino-4-substituted-1,4-dihydrobenzo[4,5]imidazo[1,2-a]pyrimidine-3-carbonitrile (Scheme 2)

In a 50-mL round-bottom flask, a mixture of 2-aminobenzimidazole **1** (2 mmol), aldehyde **2a–l** (2 mmol), malononitrile **3** (2 mmol) and 10 mol% of catalyst in water (5 mL) was heated at reflux for a specified time (Table 3). After completion of the reaction (monitored by TLC, hexane: ethyl acetate), the mixture was cooled to room temperature and then diluted with ethanol to separate catalyst from the reaction mixture by an external magnet, followed by decantation of the organic solution. The organic solution was then poured onto crushed ice to obtain solid product, which was filtered and dried. The recrystallization with ethanol afforded pure products in quantitative yields (Table 3).

Conclusion

We have developed an environmentally friendly synthetic approach for the water-mediated synthesis of 2-amino-4-substituted-1,4-dihydrobenzo[4,5]imidazo[1,2-a]pyrimidine-3-carbonitriles using newer magnetic nanocatalyst S-Chit-HAp@Fe_3O_4. Heterogeneous reaction conditions, easy separation of the catalyst after reaction by an external magnet, shorter reaction period, quantitative product yields, successful easy recovery and efficient recycling of the catalyst are worthy advantages of this greener approach.

Supplementary data

Supplementary data for this article can be accessed on the publisher's website.

Acknowledgements The authors are thankful to UGC, New Delhi, for financial assistance under a one-time grant [F. no. 19-110/2013 (BSR)] and major research project [F. no. 41-302/2012 (SR)]. the authors are also thankful to SAIF, IIT Bombay, IIT Madras and Panjab University, Chandigarh, for providing instrument facilities. Author VNM is very much grateful to the UGC, New Delhi, for awarding the Rajiv Gandhi National Fellowship.

References

1. B.B. Toure, D.G. Hall, Chem. Rev. **109**, 4439 (2009)
2. I. Ugi, S. Heck, Comb. Chem. High Throughput Screen. **4**, 1 (2001)
3. A.O. Abdelhamid, E.K.A. Abdelall, N.A.A. Riheem, S.A. Ahmed, Phosphorus Sulfur Silicon Relat. Elem. **185**, 709 (2010)
4. K. Terashima, O. Muraoka, M. Ono, Chem. Pharm. Bull. **43**, 1985 (1995)
5. S.M. Sondhi, R.P. Verma, V.K. Sharma, N. Singhal, J.L. Kraus, M. Camplo, J.C. Chermann, Phosphorus Sulfur Silicon Relat. Elem. **122**, 215 (1997)

6. T. Chiba, S. Shigeta, Y. Numazaki, Biol. Pharm. Bull. **18**, 1081 (1995)
7. S.M. Sondhi, S. Rajvanshi, M. Johar, N. Bharti, A. Azam, A. Kumar Singh, Eur. J. Med. Chem. **37**, 835 (2002)
8. S. Laurent, D. Forge, M. Port, A. Roch, C. Robic, L.V. Elst, R.N. Muller, Chem. Rev. **108**, 2064 (2008)
9. T.J. Yoon, W. Lee, Y.S. Oh, J.K. Lee, New J. Chem. **27**, 227 (2003)
10. H.H. Yang, S.Q. Zhang, X.L. Chen, Z.X. Zhuang, J.G. Xu, X.R. Wang, Anal. Chem. **76**, 1316 (2004)
11. S. Asghari, M. Mohammadnia, Res. Chem. Intermed. **43**, 7193 (2017)
12. M.J. Nasab, A.R. Kiasat, Res. Chem. Intermed. **44**, 2719 (2018)
13. J.C. Elliott, *Structure and Chemistry of the Apatites and Other Calcium Orthophosphates*, vol. 18 (Elsevier, Amsterdam, 1994), pp. 1
14. Y. Zhang, Z. Li, W. Sun, C. Xia, Catal. Commun. **10**, 237 (2008)
15. K. Huang, L. Xue, Y.C. Hu, M.Y. Huang, Y.Y. Jiang, React. Funct. Polym. **50**, 199 (2002)
16. C.C. Guo, G. Huang, X.B. Zhang, D.C. Guo, Appl. Catal. A **247**, 261 (2003)
17. J. Zhang, C.G. Xia, J. Mol. Catal. **206**, 59 (2003)
18. E. Guibal, Prog. Polym. Sci. **30**, 71 (2005)
19. D.J. Macquarrie, J.J.E. Hardy, Ind. Eng. Chem. Res. **44**, 8499 (2005)
20. H. Honarkar, M. Barikani, Monatsh. Chem. **140**, 1403 (2009)
21. M.G. Dekamin, M. Azimoshan, L. Ramezani, Green Chem. **15**, 811 (2013)
22. V.N. Mahire, P.P. Mahulikar, Chin. Chem. Lett. **26**, 983 (2015)
23. V.N. Mahire, V.E. Patel, A.B. Chaudhari, V.V. Gite, P.P. Mahulikar, J. Chem. Sci. **128**, 671 (2016)
24. V.N. Mahire, V.E. Patel, P.P. Mahulikar, Res. Chem. Intemed. **43**, 1847 (2017)
25. G. Ma, D. Yang, Y. Zhou, M. Xiao, J.F. Kennedy, J. Nie, Carbohydr. Polym. **74**, 121 (2008)
26. A. Kong, P. Wang, H. Zhang, F. Yang, S. Huang, Y. Shan, Appl. Catal. A **417**, 183 (2012)
27. X. Bian, K. Hong, X. Ge, R. Song, L. Liu, M. Xu, J. Phys. Chem. C **119**, 1700 (2015)
28. A. Shaabani, A. Rahmati, A.H. Rezayan, M. Darvishi, Z. Badri, A. Sarvari, QSAR Comb. Sci. **26**, 973 (2007)
29. X. Liu, Z. Ma, J. Xing, H. Liu, J. Magn. Magn. Mater. **270**, 1 (2004)
30. M.V. Reddy, J. Oh, Y.T. Jeong, C R Chimie **17**, 484 (2014)
31. M. Abedini, F. Shirini, M. Mousapour, O.G. Jolodar, Res. Chem. Intermed. **42**, 6221 (2016)
32. F. Shirini, M. Seddighi, O.G. Jolodar, J. Iran. Chem. Soc. **13**, 2013 (2016)
33. D. Survase, B. Bandgar, V. Helavi, Synth. Commun. **47**, 680 (2017)